Effect of Stokes Drift on HF Radar Measurements

Kenneth Laws

Department of Physics, University of California Santa Cruz

Jeffrey D. Paduan

Department of Oceanography, Naval Postgraduate School, Monterey, California

Daniel M. Fernandez

Institute of Earth Systems Science and Policy, California State University Monterey Bay, Seaside, California

The effect of non-linear wave interactions on the phase speed of Bragg-resonant gravity waves is investigated with the goal of assessing the impact on velocity estimates from HF radar systems. It is argued that this effect, termed Stokes shift, is a real portion of the phase speed measured by HF radar and that its magnitude is in the range from 0.02 m/s to 0.20 m/s, depending on radar frequency and wind speed. A formula for Stokes shift is presented and computations are made using both equilibrium wave spectra and observed directional wave spectra from Monterey Bay.

1. INTRODUCTION

The basic mechanism that allows radiowave energy backscattered from the ocean surface to be related to ocean currents is the frequency shift that results when the surface is moving relative to the receiver. Anything that moves the reflecting ocean surface will produce a Doppler shift relative to the transmitted frequency equal to

$$\Delta\omega = 2k_r c_p' = 2k_r(c_p + \Delta v_p), \qquad (1)$$

where c_p' is the phase speed of the reflector relative to the receiver and k_r is the wavenumber of the transmitted radio wave. For the resonant Bragg peak, the observed phase speed is a combination of the phase speed of the resonant waves, c_p, and any shift in that phase speed due to currents or non-linear wave interactions, Δv_p. The use of High Frequency (HF) radio frequencies in the range from 3 MHz to 30 MHz for oceanographic measurements stems from the fact that the resonant Bragg waves in this band are deep water waves whose phase speeds are precisely determined by

$$c_p = \sqrt{g/k}, \qquad (2)$$

where $k = 2k_r$ is the wavenumber of the ocean wave.

The interpretation of HF radar backscatter has generally attributed all of the residual phase shift, Δv_p, to bulk ocean currents with scales much larger than the wavelength of an individual Bragg wave, i.e., Δv_{pc}. The contributions from non-linear wave interactions, Δv_{pw}, on the other hand, have not received individual attention. It may indeed be important to identify these contributions because, should they exist, they represent a bias relative to the flow that would be detected by purely Eulerian measurement systems, such as moored current meters or Acoustic Doppler Current Profilers.

The mechanism of non-linear wave interactions leading to a mean current is commonly referred to as Stokes drift (Kenyon, 1969). It has not been clear, however, how to apply the notion of Stokes drift to alterations of Bragg wave phase speeds as detected by HF radar backscatter. Because the electromagnetic backscatter occurs at the ocean surface, does that mean that the appropriate non-linear wave interaction contribution is the Stokes drift evaluated at the surface? We suggest that this is not correct and, instead, propose that the appropriate contribution is the depth-weighted Stokes drift. In this case, the weighting function derives from the Bragg wave particle velocity as used by Stewart and Joy (1974). i.e.,

$$\Delta v_{pw} = 2k\int_{-\infty}^{0} U_S(z)e^{2kz}dz, \qquad (3)$$

where U_S is the component of the Stokes drift parallel to the radar look direction. We support this depth weighting by showing that the resulting phase speed shift due to the Stokes drift from an arbitrary wave energy spectrum is in agreement with the shift in phase speed due to higher order corrections to the dispersion relation calculated using a perturbation approach (Weber and Barrick, 1977; Barrick and Weber, 1977). The reconciliation of our approach with that of Weber and Barrick is given in the Section 2.

Sample velocity impacts are given in Sections 3 and 4 based on equilibrium wave spectra and observed wave spectra, respectively. Some conclusions from this work and suggestions for future investigations are provided in Section 5.

2. STOKES DRIFT OF BRAGG WAVES

In this section we relate the results obtained through perturbation expansions to those obtained by depth-weighting the Stokes drift formula as in (3). Details of this comparison can be found in Laws (2001). An overview of the results is provided here.

Weber and Barrick (1977) used a third order expansion of the gravity wave dispersion relation to investigate non-linear effects. They expanded the equations about the radian wave frequency, $\omega = \omega_0 + \omega_2$, to derive the phase velocity

$$v_p(\vec{k}) = \sqrt{\frac{g}{k}}\left(1 + \frac{\omega_2(\vec{k})}{\omega_0}\right). \qquad (4)$$

The factor, $\omega_2(\vec{k})/\omega_0$, is referred to as the normalized correction to the deep-water phase speed. For this perturbation expansion to be valid, the scale of the problem must be small compared to both the spatial and temporal scales of energy transfer yet large compared with the wavelengths and periods of the dominant waves present. These conditions are generally met for the spatial and temporal integration times used with HF backscatter measurements. Assuming these conditions are met, the perturbation results may be generalized to random surfaces and the mean normalized correction is given by

$$\left\langle \frac{\omega_2(k)}{\omega_0(k)} \right\rangle = \pm\int_0^k \omega_0' k' S_1(k')dk' \pm \frac{2k^2}{\omega_0}\int_k^\infty \omega_0' S_1(k')dk', \qquad (5)$$

where $S_1(\boldsymbol{k})$ is the first order approximation to the wave height spectrum $S(\boldsymbol{k})$.

We now turn to demonstrating that the current due to Stokes drift for a given wave height spectrum can be used to calculate the correction to the phase velocity of gravity waves in deep water and that, for collinear waves, the resulting phase shift approaches the second order perturbation form of Barrick and Weber. Beginning with the expression for Stokes drift at a particular depth produced by a two-dimensional ocean wave spectrum (Kenyon, 1969),

$$\vec{\boldsymbol{U}}_S(z) = \frac{1}{\rho}\int\int_{-\infty}^{\infty} S(\vec{k})\frac{\vec{k}}{\omega(k)}\left[\frac{2k\cosh[2k(z+h)]}{\sinh(2kh)}\right]d^2\vec{k}, \qquad (6)$$

where ρ is the water density and h is the water depth, we neglect the higher order corrections to the phase velocity, i.e., let $\omega \approx \omega_0 = \sqrt{gk}$, and simplify (6) as

$$\vec{\boldsymbol{U}}_S(z) = \frac{2}{\rho g}\int\int_{-\infty}^{\infty} S(\vec{\boldsymbol{k}})\vec{\boldsymbol{k}}\omega e^{2kz} d^2\vec{\boldsymbol{k}} \qquad (7)$$

for the deep water limit ($kh >> 1$). Using (7) in (3) we obtain

$$\Delta v_{pw}(k) = \frac{4k}{\rho g}\int_{-\infty}^{0} dz \int\int S(\vec{k}')(\vec{k}' \bullet \hat{x})\omega(k')e^{(k+k')2z} d^2\vec{k}'. \qquad (8)$$

Exchanging the order of integration and evaluating the integral over depth we find

$$\Delta v_{pw}(k) = \frac{2k}{\rho g}\int\int_{-\infty}^{\infty} S(\vec{k}')\frac{\vec{k}' \bullet \hat{x}}{k+k'}\omega(k')d^2\vec{k}'. \qquad (9)$$

Finally, we investigate the case of a unidirectional spectrum where the x-axis is aligned with the radar look direction to obtain

$$\Delta v_{pw}(k) = \frac{\pm 2k}{\rho g}\int_0^\infty S(k')\frac{k'}{k+k'}\omega(k')dk', \qquad (10)$$

where the positive sign is used when the wave spectrum is aligned in the same direction as the wave of interest and the negative sign is used when the spectrum is aligned in the opposite direction. Laws (2001) goes on to show that the different methods leading to (5) and (10) converge for the two regimes $k' > k$ and $k' < k$, i.e., outside the precise scale of the Bragg wave itself.

3. EQUILIBRIUM WAVE SPECTRUM RESULTS

We now examine the effect of Stokes drift on the phase speed of deep-water Bragg waves for the case in which the surface wave spectrum is in equilibrium with local wind forcing. According to Pierson and Moskowitz (1964), the equilibrium surface wave spectrum has the form

$$f_n(\omega) = (\alpha_n \rho g^3/\omega^5)e^{-\beta_n(g/W\omega)^n}, \qquad (11)$$

where

$$\alpha_n = (f_o/2\pi)(2\pi v_o)^5 e^{5/n}$$
$$\beta_n = (5/n)(2\pi v_o)^n, \qquad (12)$$

W is the wind speed, f_o = 2.75 x 10^{-2}, and v_o = 0.140. Assuming n = 4 (Pierson and Moskowitz, 1964), the wave energy spectrum is given by

$$E_4(\nu,\theta) = (2\pi/\rho g) f_4(\omega,\theta) \bullet G(\theta), \quad (13)$$

where $\nu = \omega/2\pi$ is the frequency in cycles/sec, θ is the angle with respect to the wind vector, and $G(\theta)$ represents a directional spreading model. For simplicity, we investigate the maximum effect, which is aligned with the wind. For this case, $G(\theta) = G(0) = 1$. Downwind, equilibrium spectra are shown in Figure 1 for three different wind speeds. For higher wind speeds the energy peak shifts to lower frequencies, which moves the period of the dominant waves up from about 7 sec to 10 sec for the range of wind speeds shown here.

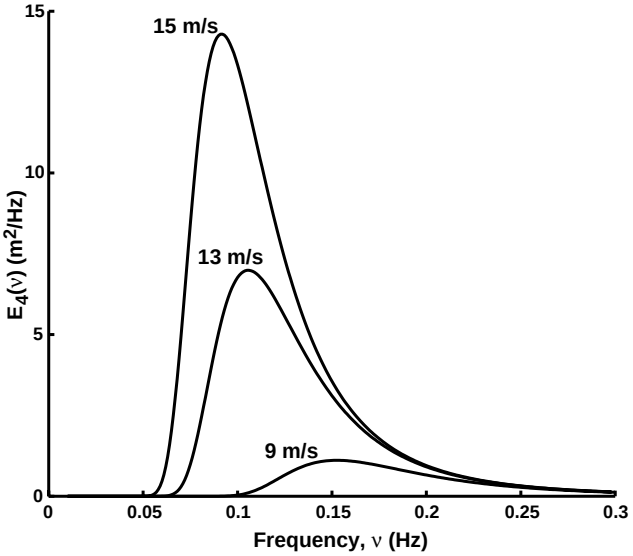

Figure 1. Theoretical downwind wave energy spectra for fully developed seas in equilibrium with wind speeds of 9 m/s, 13 m/s, and 15 m/s.

Using the equilibrium spectra in (7), it is possible to, numerically, evaluate the downwind Stokes drift as a function of depth for different wind speeds. Those results are shown in Figure 2 for the range of winds used in Figure 1. At the lower wind speed of 9 m/s, which is typical of the conditions over Monterey Bay, Stokes drift values range from 0.23 m/s at the surface to near zero at 10 m depth. For waves in equilibrium with wind speeds of 15 m/s, surface Stokes drift currents rise to 0.35 m/s.

It is interesting to assess which portion of the wind wave spectrum provides the largest contribution to Stokes drift. This too was investigated numerically by continuously increasing the range of frequencies included in the integral in (7). These results are shown in Figure 3 at three different depths for the 15 m/s wind speed case. From Figure 1 it can be seen that the wave spectra peaks near 0.10 Hz for this case and the energy is down below the half power point at frequencies above 0.15 Hz. Despite this, frequencies below 0.15 Hz account for only 65% of the Stokes drift at 2 m depth and only 35% of the Stokes drift at the surface. Because of the strong frequency weighting in these calculations, the higher frequencies contribute more to Stokes drift than might be expected from the spectral shapes.

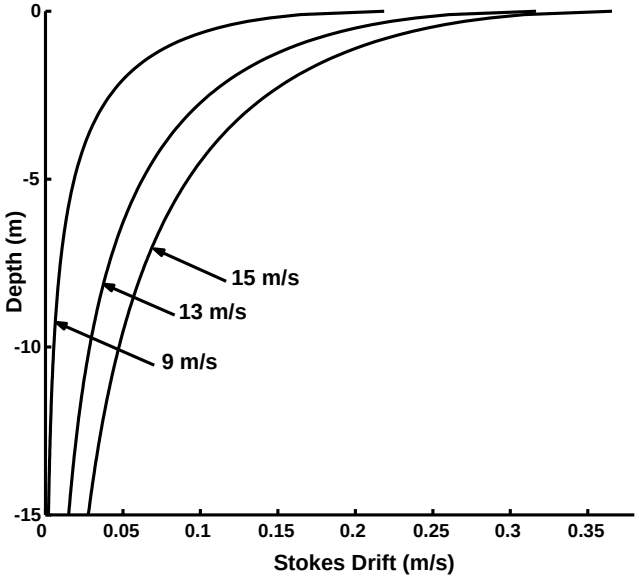

Figure 2. Downwind Stokes drift as a function of depth for waves spectra in equilibrium with wind speeds of 9 m/s, 13 m/s, and 15 m/s.

Finally, we use the equilibrium wave spectra to assess the magnitude of the phase speed shift for Bragg waves due to Stokes drift, which we term the "Stokes shift." Using (7) in the depth weighting formula (3), we obtain the following formula for Stokes shift under equilibrium wave conditions (see Laws, 2001 for details):

$$\Delta v_{pw}(k) = \frac{16\pi^3 k}{g} \int_0^{2\pi} \cos\theta d\theta \int_0^{\infty} \left(\frac{\nu^3}{4\pi^2\nu^2/g + k} \right) E(\nu,\theta) d\nu. \quad (14)$$

Equation (14) was evaluated for the range of equilibrium wind speeds used above and the results are presented in Figure 4 as a function of Bragg wavenumber. For reference, the four wavenumbers associated with the different frequencies used by the Multi-frequency Coastal Radar (MCR; Teague et al., 2001) system are denoted on the figure. All commonly used HF radar system frequencies fall close to one of the MCR frequencies. The Stokes shift ranges from 0.12 m/s to 0.27 m/s over the wind speed range for the higher radar frequency (21.8 MHz). At the lowest radar frequency (4.8 MHz), the Stokes shift ranges from 0.07 m/s to 0.13 m/s for the same range of wind speeds. The effect due to Stokes drift is larger on the higher frequency Bragg waves because their depth weighting function is trapped more closely to the surface.

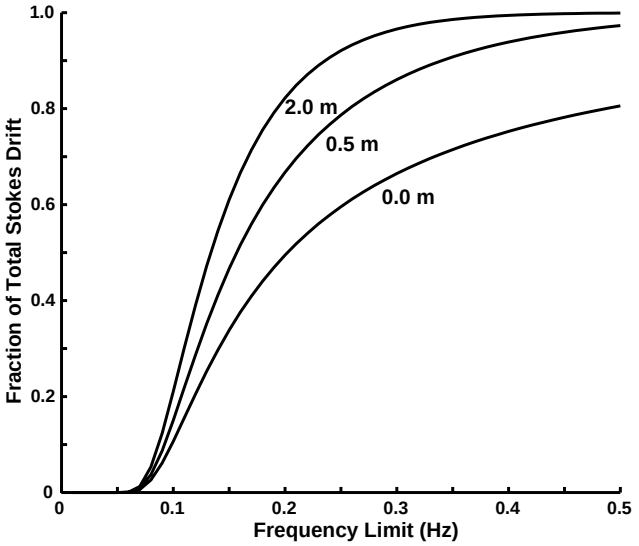

Figure 3. Fraction of total Stokes drift as a function of the upper frequency limit for waves in equilibrium with a wind speed of 15 m/s at the surface, 0.5 m depth, and 2.0 m depth.

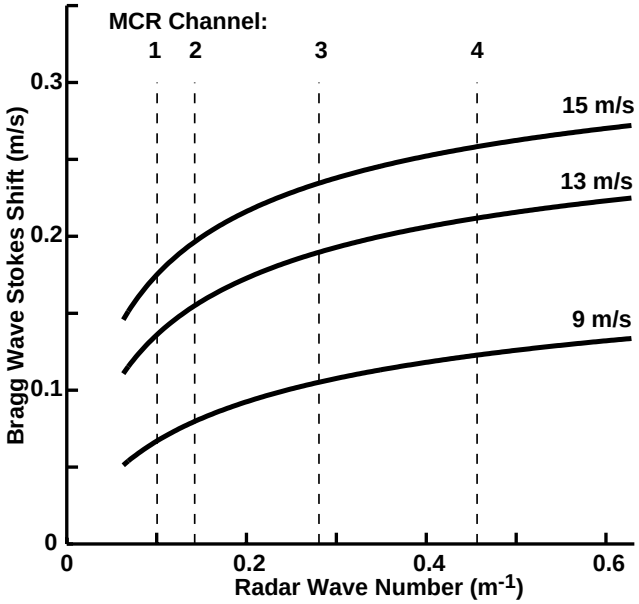

Figure 4. Shift in phase speed of Bragg resonant waves due to Stokes drift as a function of radar wave number for wave spectra in equilibrium with wind speeds of 9 m/s, 13 m/s, and 15 m/s. The dashed lines denote wave numbers corresponding to the four frequencies of operation for the MCR system: CH1 (4.8 MHz), CH2 (6.8 MHz), CH3 (13.4 MHz), and CH4 (21.8 MHz).

4. OBSERVED WAVE SPECTRUM RESULTS

The equilibrium wave spectra used in Section 3 may not always reflect the actual directional wave spectrum, particularly near the coastline where fetch can be limited. However, simultaneous measurements of HF backscatter and wave spectra from which Stokes shift can be computed are not common. We report results from one particular data set in this section, which was collected in Monterey Bay between 3 September and 11 November, 1999. Again, more details may be found in Laws (2001).

During the Fall 1999 period, MCR data were collected from two locations around Monterey Bay. At the same time, a flux buoy was deployed in the Bay by the Department of Meteorology at the Naval Postgraduate School. The locations of the radar sites and buoy are shown in Figure 5. The unique aspects of this data set are the multi-frequency data collected by the MCR systems and the combination of bulk wind, direct wind stress, and directional wave data collected by the flux buoy.

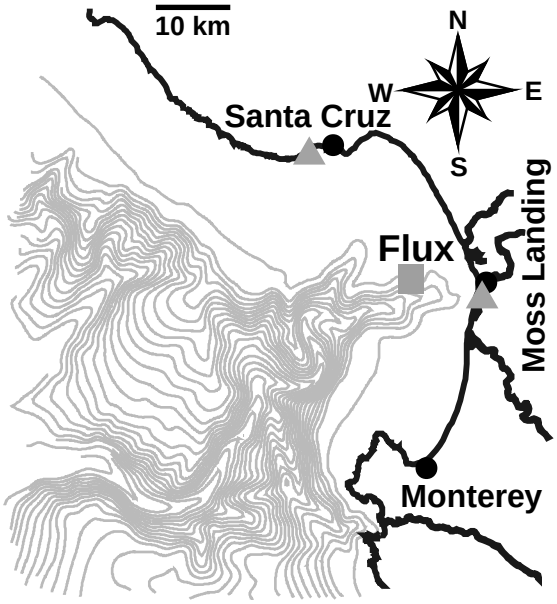

Figure 5. Location of MCR HF radar sites (triangles) and moored flux buoy in Monterey Bay during Fall 1999.

Given directional wave spectra, the vector Stokes shift may be computed directly using (9). The magnitude and direction of the computed shift for the Bragg waves associated with the highest MCR frequency (21.8 MHz) are shown in Figure 6. The magnitude was typically below 0.02 m/s during this period with short-duration peak values up to 0.08 m/s. The magnitudes for Bragg waves associated with lower radar frequencies would have been even smaller. The direction of the vector Stokes shift was typically toward the east-southeast reflecting the onshore wave conditions at the flux buoy location.

The wind speeds measured at the flux buoy during this period (not shown) were weak. Most days winds exhibited a clear diurnal cycle with speeds between 2 m/s and 6 m/s. The strong event on year day 280 had peak speeds of 13 m/s. Comparing the computed Stokes shift in Figure 6 with the theoretical values in Figure 4 based on equilibrium wave spectra we see that the observed values were about half as large as the equilibrium values, which suggests that the observed wave field at the flux buoy was not in equilibrium with the local winds. This result can be seen more clearly in direct comparisons of the observed

and equilibrium spectra (not shown). Individual wave spectra were examined to determine whether the spectral contributions to Stokes shift from the observed waves were similar to what was found for the equilibrium cases even though the energy levels were lower. One example was taken from the wave event on year day 301, which is denoted on the time series in Figure 6. The two-dimensional wave spectrum was collapsed into a single dimension by plotting the peak energy at each frequency in Figure 7. The highest overall energy levels were for waves with periods longer than 10 seconds, which includes the contributions from swell.

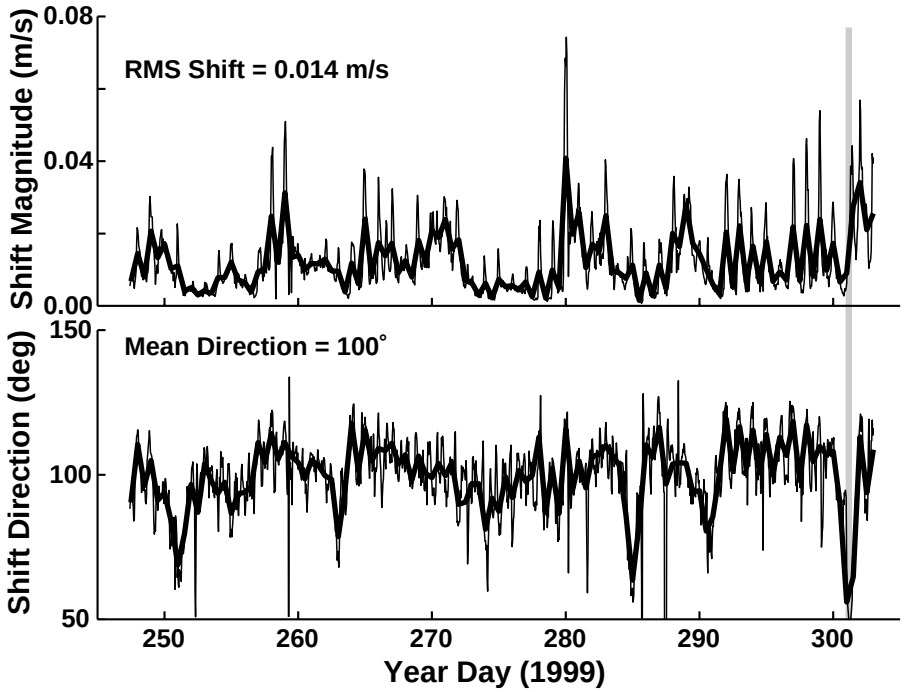

Figure 6. Magnitude and direction (toward) of the Stokes shift for Bragg waves resonant with 21.8 MHz radiowave signals calculated from observed directional wave spectra at the flux buoy in Monterey Bay. The heavy line denotes a 12-hr running average and the vertical bar denotes the period of the example spectrum.

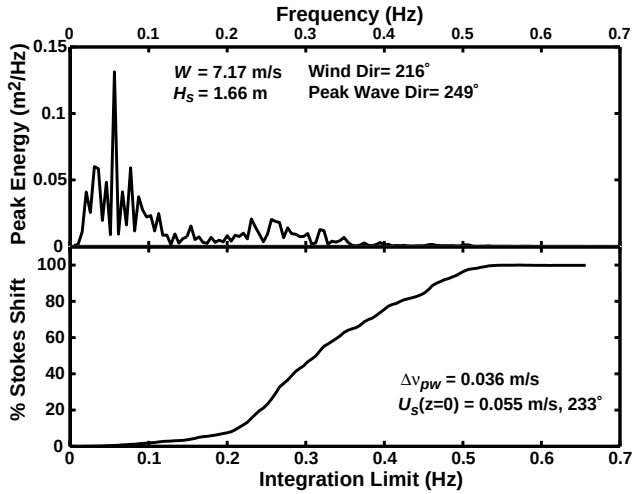

Figure 7. Wave energy density as a function of frequency (upper panel) and the fraction of total Stokes shift for Bragg waves resonant with 21.8 MHz radiowave signals as a function of upper frequency cut-off (lower panel).

The spectral information in Figure 7 also shows the cumulative contributions to the total Stokes shift as a function of the upper wave frequency limit. It is even more apparent in this non-equilibrium example that the shorter wind waves dominate the Stokes shift calculation with most of the contribution coming from waves with periods less than 5 seconds.

The small Stokes shift values computed from this data set are well within typical noise levels of the HF radar systems. For this reason it is difficult to verify that the proposed Stokes shift formula is correct based on field observations. If the Stokes shift effect were larger, it would be expected to be correlated with the HF radar-derived radial velocities. A complicating factor is that the waves can be strongly correlated with wind, which itself is correlated with near-surface current. Laws (20001) presents the comparisons between observed currents and Stokes shift for all MCR frequencies. He also investigates the correlation between currents and wind or wind stress. Because the currents are relatively weak in this data set and the signal-to-noise performance of the MCR systems was relatively poor during that period, the results of these comparisons are not conclusive. The situation is improved, somewhat, when the unique multi-frequency aspect of the MCR data is exploited to compare near-

surface shear to the computed Stokes shift and observed wind and wind stress records.

An estimate of near-surface shear near the location of the flux buoy was created by taking the difference of radial velocities measured at 21.8 MHz and 4.8 MHz. Only data along the radial direction from the Santa Cruz MCR site were used due to extremely poor range performance from the system at Moss Landing during this period. The radar-determined velocity difference represents shear in the upper 2 m. The precise depth difference depends on details of the velocity profile near the ocean surface (Stewart and Joy, 1974; Ha, 1979; Teague et al., 2001; Teague et al., this issue). It is likely, however, that many physical processes have vertical scales large compared with the 1 m scale of the shear calculation. Examples include tidal currents, geostrophic currents, and, to an unknown extent, directly wind-driven currents.

Comparison of the radar-derived velocity difference and computed difference in Stokes shift for the two different Bragg waves is given in Figure 8. The velocity difference data is also compared with wind speed, wind speed squared, and friction velocity. (The latter was directly measured on the flux buoy using turbulent eddy correlation sensors independent of the wind measurements.) In these comparisons, the complex correlation of the vector Stokes shift difference, wind, or friction velocity against the (scalar) velocity difference was computed. The correlation results presented in Figure 7 represent the magnitude of the complex correlation and the scatter plots represent the direction parallel to the correlation phase angle. The correlation values are similar for Stokes shift difference and wind or wind stress. The best correlation overall was between velocity difference and wind stress (friction velocity). Hence, even though these results show some skill in predicting radar-derived velocities using the wave-based Stokes shift formula, they do not rule out the possibility that a strong correlation between winds and waves is responsible.

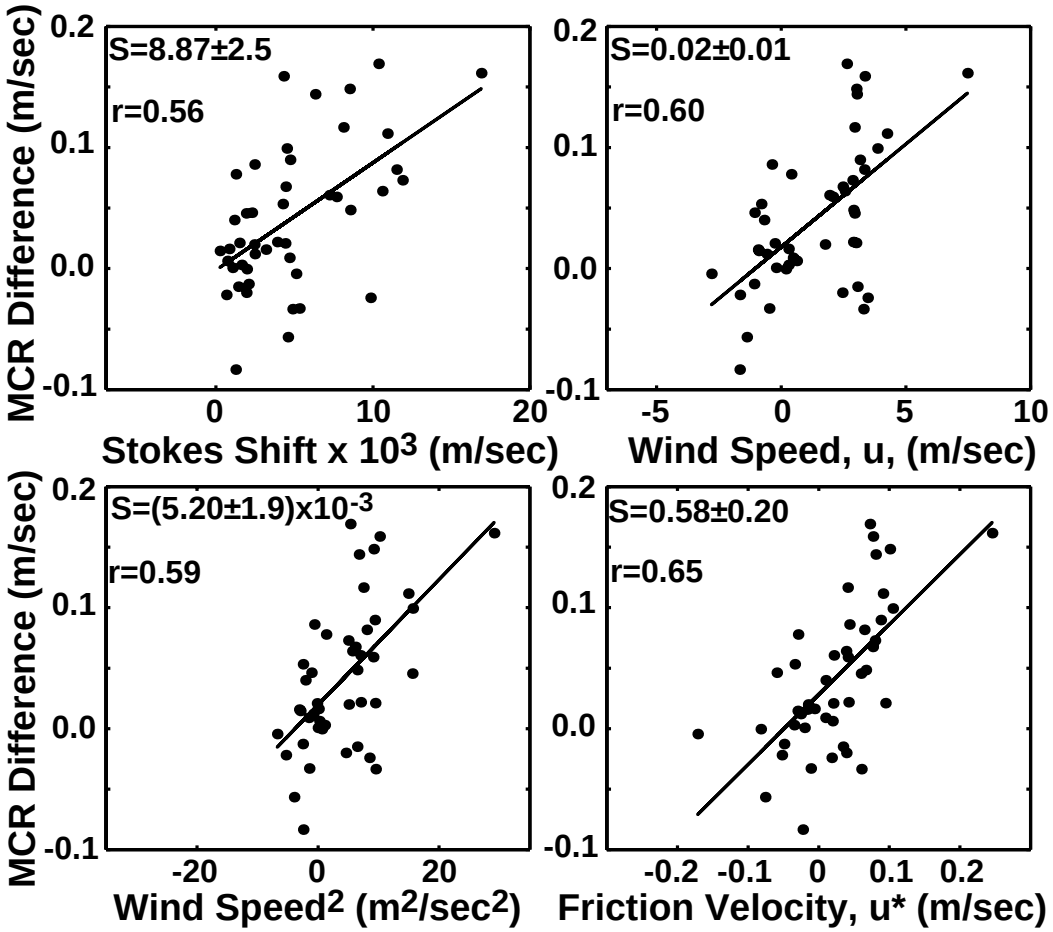

Figure 8. Difference between radial velocities from the MCR system in Santa Cruz measured at 21.8 MHz and 4.8 MHz for the location of the flux buoy in Monterey Bay during Fall 1999 compared with difference in Stokes shift for the two frequencies based on directional wave data from the flux buoy and with wind speed and wind speed squared projected onto the radar look direction and friction velocity measured on the flux buoy. The complex correlation magnitude (r) is shown for each comparison along with the slope (s) of the regression measured parallel to the correlation phase angle.

5. CONCLUSIONS

This work has investigated the effect on non-linear wave interactions on the measurement of ocean currents by HF radar backscatter techniques. Analytical work was presented here that reconciles two independent derivations of the expected Bragg wave phase shift: one based on the perturbation method of Weber and Barrick (1977) and one proposed by Laws (2001) in which the classic Stokes drift current of Kenyon (1969) is integrated over depth weighted by the Bragg wave particle velocities as proposed by Stewart and Joy (1974) for the general effect due to a near-surface velocity field. Both of these approaches argue for the existence of a detectable, wave-driven perturbation to the deep-water Bragg wave phase speed, which should, therefore, be part of the signal detected by HF radar systems.

The magnitude of the wave-related biases was estimated in two ways. First, computations were done using the equilibrium wave model and a range of wind speeds that suggest current biases on the order of 0.10 m/s for typical wind speeds on the order of 10 m/s. Next, the expected velocity biases were computed from directional wave spectra measured in Monterey Bay in Fall 1999. In that case, the Stokes shift effect was about five times weaker, which was due to low winds and, apparently, non-fully developed sea states.

The effort presented here to extract the wave-related portion of radial currents measured in Monterey Bay was not convincing. Significant correlation was seen between the wave-estimated Stokes shift and the radar-derived current, but even stronger correlation was found between the wind stress and the current. In the future, additional data sets with simultaneous HF radar and directional wave data should be analyzed for the effect of wave-induced velocities. This is important because these effects represent a bias between HF radar-derived current measurements and those of other current meters that is a large fraction of the typical 0.07 m/sec to 0.15 m/sec uncertainty levels (Graber et al., 1997, Paduan and Rosenfeld, 1996). It is also important because numerical circulation models that, increasingly, use HF radar-derived currents as validation or assimilation data sources do not include this wave effect. Hence, it should be removed from the data set prior to model-data comparison or data assimilation (or incorporated into the error covariance descriptions). Prior to definitive measurements of the non-linear wave effects on HF radar measurements, we believe that the formula presented here could be used with directional wave data or, if necessary, with wind data to estimate the Stokes shift for a given data set.

Acknowledgments. This work was supported by NSF grant OCE-9731304 to the Naval Postgraduate School. Data from the flux buoy were provided by K. Davidson under ONR grant N00014-00-WR20098 to the Naval Postgraduate School. The authors thank D. Barrick and J. Vesecky for many helpful discussions.

REFERENCES

Barrick, D.E., and B.L. Weber, On the nonlinear theory for gravity waves on the ocean's surface. Part II: Interpretation and applications. *J. Phys. Oceanog.*, 7, 11-21, 1977.

H. C. Graber, B. K. Haus, R. D. Chapman, and L. K. Shay, Journal of Geophysical Research 102, 18749 (1997).

Ha, E.C., Remote sensing of ocean surface current and current shear by HF backscatter radar. PhD thesis, Tech. Rep. D415-1, Stanford University, Stanford, Calif., 134pp., 1979.

K. E. Kenyon, Journal of Geophysical Research 74, 6991 (1969).

Paduan, J.D., and L.K. Rosenfeld, Remotely sensed surface currents in Monterey Bay from shore-based HF radar (CODAR). *J. Geophys. Res.*, 101, 20669-20686, 1996.

W. J. Pierson and L. Moskowitz, Journal of Geophysical Research 69(24), 5181 (1964).

Stewart, R.H., and J.W. Joy, HF radio measurement of surface currents. *Deep-Sea Res*., 21, 1039-1049, 1974.

Teague, C.C., COPE3 paper. *J. Oceanic Engin*., in press, 2001.

Teague et al., this issue

Weber, B.L., and D.E. Barrick, On the nonlinear theory for gravity waves on the ocean's surface. Part I: Derivations. *J. Phys. Oceanog*., 7, 3-10, 1977.

D.M Fernandez, ESSP, California State University Monterey Bay, 100 Campus Center, Seaside, CA 93955

K. Laws, Dept. of Physics, University of California, Santa Cruz, CA 95062

J.D. Paduan, Code OC/Pd, Naval Postgraduate School, Monterey, CA 93943 (email: paduan@nps.navy.mil)